Proceedings of the American Society of Mechanical Engineers (ASME)
2006 International Solar Energy Conference (ISEC 2006)
July 8-13, 2006 Adam's Mark Hotel, Denver, Colorado, USA

ISEC2006-99168

UNCERTAINTY CALCULATIONS IN PYRANOMETER MEASUREMENTS AND APPLICATION

M.G. Kratzenberg [1], H. G. Beyer [2], S. Colle [1], A. Albertazzi [3]

[1] Solar Energy Laboratory, Federal University of Santa Catarina,
Department of Mechanical Engineering, Florianópolis, Brazil

[2] Institute of Electrical Engineering, University of Applied Sciences Magdeburg-Stendal,
Magdeburg, Germany

[3] Laboratory of Metrology and Industrial Automation, Federal University of Santa Catarina,
Department of Mechanical Engineering, Florianópolis, Brazil

ABSTRACT

The uncertainty of pyranometer measurements should be traced back to the World Radiation Reference (WRR), a standard that is specified by the mean sensitivity of the World Standard Group (WSG). The WSG is build up by 7 primary standard pyrheliometers, operated at Davos, Switzerland. Analyzing the complete calibration chain for an individual field pyranometer, usually the uncertainty of its calibration constant is extracted as a unique figure depending on the calibration method. The common representation of the expanded uncertainty, specified by the manufacturer is global information on the *accuracy* of daily averages.

For the use of pyranometers for e.g. test of solar energy components as solar collectors, this information on the global daily accuracy of the pyranometer is not sufficient. As the response of a solar collector to the irradiance shows nonlinearities, a more detailed analysis of the pyranometer uncertainties is necessary.

This will be demonstrated for the analysis of the uncertainties of the test results - i.e. the collector coefficients and their uncertainties - and the resulting predictions of the energy gain by these devices. Ancillary information by the manufacturers will be used to discuss the uncertainty of individual measurements depending on e.g. ranges of those parameters that originate the uncertainties, depending on the geometry (incidence angle), ambient temperature and the sky conditions. Based on this information the inter-comparability of test performed at different times or with different instruments will be discussed.

INTRODUCTION

The model of a solar thermal collector has to describe its efficiency as function of irradiance, ambient and operational temperatures. Using standard model structures, individual collectors are characterized by a set of collector model parameters, determined by the regression coefficients. For to determining these parameter sets several procedures are proposed, each relying to a specific model structure.

Actually the most used outdoor collector test is the SST collector test that is normalized by the ISO9806 [1], EN12975 [2] and ASHARE 93-86[3].

Alternatively the European standard EN12975 specifies a quasi dynamic collector test (QDT) referring to a more detailed dynamic collector model. This model is an extended version of the model corresponding to the SST. The QDT model explicitly addresses the response characteristics of a solar collector to the solar broadband beam and diffuse radiation, the solar incidence angle to the collector normal and the ambient temperature. The QDT model is able to handle a higher variability of meteorological conditions so that the QDT test needs less time to collect the data base sufficient for the parameter evaluation. This leads to a shorter duration of the test and improves its accuracy [4].

In the QDT collector test, a major contribution to the uncertainties is caused by the transducers for the solar irradiance i.e. the pyranometers [4] showing both, systematic and random errors. The random errors of the regression variables, connected to the irradiance measurements, as well as those for temperature and mass flow measurements are transformed by the regression process in the random

uncertainties of the collector coefficients [5] and are interpreted as the homoscedastic uncertainties of the model response of the collector model [4]. The systematic errors that remain after the calibration process have to be interpreted as additional systematic uncertainties appearing in both, the QDT and SST collector test. This is caused by the fact that the uncompensated part of systematic uncertainty that is e.g. a function of the ambient temperature can create additional uncertainties. This effect has to be taken into account e.g. in case that two different collector tests, using the same collector, are accomplished under different ambient temperatures. In [15] it is shown that most of the pyranometer errors, as specified by the manufacturer, have both, a random and a systematic part. As the random contribution to the error of the pyranometers is not known, we assume for a worst case calculation, all the specified [6] pyranometer errors are systematic errors.

The manufacturer of the pyranometers usually specifies the maximal uncertainty interval - composed of both, random and systematic errors – as a function of the operation conditions of the pyranometers [6] and specifying the absolute, relative and offset errors of the pyranometers [6].

The errors specified by the manufacturer are considered as gross values of the uncertainties (Table 1 and Table 2, see below).

As EN12975 requires, for the measurement of the global and the diffuse irradiance two uncertainty budgets have to be analyzed here. In the uncertainty budgets all the specified pyranometer uncertainties are combined and the expanded uncertainties [7] are determined for the reference values for the global radiation of 800 W/m^2 and the diffuse radiation of 120 W/m^2. The expanded pyranometer uncertainties are calculated for the different operation conditions of the pyranometers and are added to the uncertainty interval of the QDT collector efficiency curve.

CONTRIBUTIONS TO THE UNCERTAINTY BUDGET DUE TO THE MEASUREMENTS OF THE GLOBAL IRRADIANCE

To give a clear view of the uncertainty budget of the irradiance measurements, the different contributions to the expanded uncertainty are listed in the following, first for the global irradiance. As in the framework of the standardized analyses of solar thermal collectors a global irradiance of 800 W/m² is taken as reference value, uncertainties are discussed for that irradiance level.

Repeatability

In [5] the repeatability is specified as the degree of concordance in between the results of succeeded measurements of a quantity. The repeatability is a random effect and is thus implicitly included in the uncertainty of the regression results. It does not have to be included in the present uncertainty budget, as the random effects of the errors of the measurement instruments, specified as random transducer uncertainties [7], are transformed by the regression process to uncertainties of the regression coefficients [5]. Within the calibration of the pyranometer or e.g. the measurement of a not varying quantity the repeatability has to be taken into account.

Aliasing uncertainty

Additional uncertainty has to be considered if the measuring frequency is below the Nyquist frequency [8]. To assess the aliasing effects [8], global irradiance was measured during 3 weeks with a measuring interval of 1 s and analyzed for fluctuations. No frequencies higher than 0.0025 Hz were observed. The sampling theorem [8] states that the sample frequency has to be greater than the Nyquist frequency that is twice the highest frequency observed in the measured signal. Thus the measuring interval has to be lower than 200 s. EN12975 specifies the maximum measuring interval with 6 s so that aliasing effect can not cause considerable uncertainties in the measurement.

Calibration uncertainties (Cal)

For pyranometer calibrations different methods are suggested by different institutions. In [9] the simplest *comparison calibration* method for field pyranometer is specified. In [21] the *alternating sun-and-shade* (ASSM) method and; as extension, the *continuous sun-and-shade* (CoSSM) are described. The specification of the latter one, where the pyranometers are calibrated under clear sky conditions and the reference global solar irradiance is calculated as the sum of two reference components, the diffuse and the beam solar irradiances, was improved and denominated *NREL component summation* method [29]. In [22] *sun-and-shade* and *NREL component summation* are combined to minimize the offset error for the calibration of pyranometers that are used to measure the diffuse radiation. The standard procedure for the calibration of pyranometers adopted by the Baseline Surface Radiation Network (BSRN), an institution of the World Meteorological Organization (WMO), is that of Forgan (1996) [23]. Since with the *continuous sun-and-shade* method or the *NREL component summation* method it is possible to calibrate several pyranometers at the same time, this method seams to provide a good compromise in the relation of cost and benefit. Independent of the choice of the calibration method, the obtained calibration uncertainty (first line in table 1 and table 2) - which may be different for each calibration method - has not to increase the expanded measuring uncertainty (last line in table 1 and table 2), beyond the allowed limit. The ISO9806 specify this limit with ± 50 W/m^2; the EN12975 is not specifying a limit but determines the pyranometer as secondary standard pyranometer that is the highest standard in [14]. The secondary standard specifies the maximal pyranometer uncertainties during its operation with the same intervals as specified by the *high quality* classification, the classification with lowest uncertainty specifications in [30].

The expanded uncertainty value of a measurement with the pyranometers has to be based on a calibration chain that can guaranty the traceability to the WRR. In our application the calibration uncertainty, traceable to the WRR, was obtained by the *comparison calibration* with 3.03 % [9], whereby the hierarchy of the traceability of the reference pyranometer in this calibration is specified in [24]. For a global irradiance of 800 W/m^2 this gives an uncertainty of 22.32 W/m^2.

Long term drift or stability of the transducer (DtPa)

If we considered one new calibration of the pyranometer each year, we obtain a relative uncertainty of ± 0.5% according to

the specification of the manufacturer [6]. This corresponds to 4 W/m^2 at a global irradiance of 800 W/m^2 (the maximal stability error is specified in [14] and [30] with ± 0.8% for the considered secondary standard pyranometer and the high quality classification).

Directional response error as a function of the azimuth and zenith angle (Rd)

The directional error is specified as the combined cosine and azimuth responsivity variations [20],[6] and depends on imperfections of the glass dome and the angular reflection properties of the black paint [6]. The manufacturer specifies the maximal relative zenith response error in any azimuth direction, which represents the combination of these two errors, of a horizontally mounted pyranometer as a function of the zenith angle [6, Figure 9]. For tilted pyranometers the zenith angle can be substituted with the incidence angle of the direct irradiance to account the zenith responsivity error.

As we limit our analysis to incidence angles below 60° - which is motivated by limitations in the application intended (the QDT model used for characterizing the collector (see below) has a limited reliability for incidence angles above 60° [10]) - we apply the information given by the manufacturer for the bidirectional zenith response error of the pyranometer specified for incidence angles in the range of (0 to 60)°[5]. This value is given as ± (0 to 2) % [6, Figure 9]. For higher zenith angles the pyranometer presents higher errors (e.g. 6% for 80°). The maximal directional error is specified with ± 10 W/m^2 for a beam of 1000 W/m^2 ([6] for the CM11 pyranometer; [14], [30] for the considered secondary standard pyranometer or the high quality classification) that is used for the uncertainty budget. Observation: Analyzing the measured data we observed for incidence angles of 40° maximal radiations of 900 W/m^2 that corresponds with ± 1 % [6, Figure 9] to 9 W/m^2 and for incidence angles of 60° we observed maximal radiation intensities of 550 W/m^2 that results in 11 W/m^2 with ± 2 % [6, Figure 9].

Offset caused by the long wave radiation from the sky (OS I)

This effect gives an uncertainty of ± 7 W/m^2 at a thermal net radiation of 200 W/m^2 (in [14] and [30] is given the same specification).

Offset caused changes of the ambient temperature (OS II)

The manufacturer specifies an offset with ± 2 W/m^2 given a gradient of 5 K/hr in ambient temperature for the CM11 transducer (in [14] and [30] is given the same specification).

Temperature dependence of the sensitivity (Dter)

For ambient temperatures of (0 to 40) °C the manufacturer specifies the maximal temperature error in ± 1 %. Relating this error to the global radiation of 800 W/m^2, we obtain an error of ± 8 W/m^2 (the maximal temperature error is specified in [14] and [30] with ± 2 %).

Non linearity (NL)

The manufacturer specifies the non linearity of the pyranometer in the range of (0 to 1000) W/m^2, with ± 0.6 % that corresponds to ± 4.8 W/m^2 at 800 W/m². The calibration of the pyranometer was done with a mean radiation of approximately 800 W/m^2, so that for this radiation the uncertainty based on the non linearity tends to be zero. As in the QDT basically the whole measuring range is used (300 to 1100) W/m^2, we estimate conservatively the ± 6.5 W/m^2 as uncertainty (the maximal change originated by the non-linearity of the pyranometer is specified in [14] and [30] with ± 0.5% for the radiation range of (100 to 1000) W/m^2 .

Spectral response (Es)

The manufacturer [6] does not specify an uncertainty of the spectral response, but gives a plot of the reflectance of the carbon black painted disc of the CM 11 type pyranometer as a function of the wavelengths for the range (0.25 to 2.5) μm. In this range, the reflectance varies from (2 to 3.5) %. In [15] a detailed analysis evolving the *MODTRAN4 atmospheric spectral radiative transfer model* [25] assesses the uncertainty caused by the variation of the responsivity of a secondary standard pyranometer that results in 0.5%.

Thus we consider a spectral uncertainty of ± 0.5 %, assuming small spectral variability's for different solar radiation compositions. Relating this uncertainty to the global radiation of 800 W/m^2, we obtain an error of ± 4 W/m^2 (the maximal variations of the spectral sensitivity is specified in [14] and [30] with ± 2 %).

Tilt response error (MIn)

The tilt response error is specified by the manufacturer with ± 0.2 % corresponding to 1.6 W/m^2 for (0 to 90) ° tilt angles. (in [14] and [30] this error is specified with ± 0.5 % for 1000 W/m^2).

Long term drift of the measuring unit HP34970A (DtSt)

If we consider one calibration of the HP34970A each year, we expect an error of 0.01 % relative to the measured value and 0.001 % relative to the end of the range [13], according manufacturer specification. For a maximum output voltage of the pyranometer CM11 of 6 mV and for the measurement range of 100 mV of the HP34970A, we obtain (0.6 and 1) μV, respectively as errors. These is transferred to solar radiation uncertainties of (0.12 and 0.2) W/m^2, resulting in 0.32 W/m^2.

Resolution of the measuring unit HP34970A

The resolution of the datalogger HP34970A is specified with $6^{1/2}$ digits by the manual of the datalogger. That corresponds to 0.0001%. The maximal truncation error corresponds to the half of the value of the resolution, giving ± 0.05 μV at a full range of 100 mV. With the sensitivity of the pyranometer (typically 6 to 8 μV W^{-1}m^{-2}) this gives the gross value of the uncertainty of 0.01 W/m^2 for the resolution. As very high resolution originates only random uncertainties, it has not to be considered in the systematic uncertainty calculation.

Error of the A/D converter of the HP34970A (A/D)

For the calibration interval of one year the manufacturer specifies for the analog to digital converter two errors that are 0.0002 % of measured value and 0.001 % of the end of the used measuring range of the HP34970A [13]. The errors corresponding to (0.01 and 0.1) μV if we relate the errors to the maximal voltage of 6 mV of the pyranometer and the end of range voltage of 100 mV of the HP34970A. Dividing the

sensibility coefficient of the pyranometer to this voltages, we obtain (0.002 and 0.02) W/m^2, that sums to 0.0202 W/m^2.

EVALUATION OF THE UCERTAINTY BUDGETS FOR THE GLOBAL AND DIFFUSE IRRADIANCE

Table 1 and Table 2 shows the uncertainty budget determined for the magnitude of the global solar radiation of 800 W/m^2 and diffuse radiation of 120 W/m^2 that are specified by the EN12975 for the normalized efficiency curve. ISO-GUM determines the divisor of the gross value of the uncertainty to obtain the standard uncertainty that is 2 for normal distribution considerations and $\sqrt{3}$ for uniform distribution considerations. The normal distribution of the calibration uncertainty can be used for uncertainty budget of the calibration. The uniform uncertainty distribution - a more conservative consideration - has to be used whenever the distribution of the uncertainty is unknown [5]. All the unknown and thus uncorrectable systematic effects have to be accounted in the uncertainty budget together with the random effects [5].

The combined standard uncertainty [5] is calculated by the following equation

$$u_c = \sqrt{u_1^2 + u_2^2 ... u_n^2} \qquad (1)$$

Where u_1 to u_n are the calculated standard uncertainties.
The combined uncertainty is used to calculate the expanded uncertainty [5] of a measurement using the following equation

$$U = t_{\alpha/2,n-1}\, u_c \qquad (2)$$

The $t_{\alpha/2,n-1}$ factor to calculate the expanded uncertainty [5] of a two sided confidence interval can be extracted from the *student's-t distribution table* using ν_{eff} = n-1 effective degrees of freedom, determined by the following equation

$$\nu_{ef} = \frac{u_c^4}{\left(\frac{u_1^4}{\nu_1} + \frac{u_2^4}{\nu_2} + ... \frac{u_n^4}{\nu_n}\right)} \qquad (3)$$

Where (ν_1 to ν_n) are the degrees of freedom for the uncertainty components. For uniform distributions they are considered as infinity e.g. $\nu_{eff} = \infty$.

The degrees of freedom used for the calibration uncertainty come from the uncertainty budget of the calibration process [4].

As the random effects of the used transducers are interpreted by the regression uncertainties, in the uncertainty budgets only the systematic errors with not known characteristics of the pyranometers (Table 1 and Table 2) are taken into account. The systematic uncertainties with known characteristic, which were corrected with a correction model, were listed in the uncertainty budget.

Table 1: Uncertainty budget for the measurement of the global radiation of 800 W/m2 with the CM11 pyranometer

origin of the uncertainty		systematic corrections with a model	not corrected systematic uncertainties				
symbol	description of the uncertainty		gross value [W/m²]	distribution form	divisor	u [W/m²]	ν
Cal	Calibration uncertainty		22.32	normal	2.00	11.16	∞
DtPa	Drift over time (change / year)		4.00	uniform	1.73	2.31	∞
Rd	Directional response (as a function of the azimuth and the zenith angle)		10.00	uniform	1.73	5.77	∞
OS I	Offset originated by the thermal radiation		7.00	uniform	1.73	4.04	∞
OS II	Offset originated by the temperature change		2.00	uniform	1.73	1.15	∞
Dter	Temperature dependence of the sensitivity		8.00	uniform	1.73	4.62	∞
NL	Non linearity		6.50	uniform	1.73	3.75	∞
ReE	Spectral response		4.00	uniform	1.73	2.31	∞
MIn	Tilt response		1.60	uniform	1.73	0.92	∞
DtS	Long time drift of the measuring system		0.32	uniform	1.73	0.18	∞
A/D	Error of the analog to digital converter of the measuring unit		0.02	uniform	1.73	0.01	∞
	Combined standard uncertainty			**normal**		**14.92**	∞
	Expanded standard uncertainty			**normal**		**29.83**	

CONTRIBUTIONS TO THE UNCERTAINTY BUDGET OF THE MEASUREMENT OF THE DIFFUSE IRRADIANCE

This section discusses the contributions to the uncertainty of the measured diffuse irradiance. Here the uncertainties are calculated for the diffuse radiation of 120 W/m^2. It should be noted, that in practice global and diffuse irradiance are measured by separate instruments, a fact that later on has to be taken into account when discussing the influence of the uncertainties in measured irradiances in the context of applications.

Calibration uncertainties (Cal)
Based on the same simple comparison calibration at the same magnitude of global radiation, the relative calibration uncertainty of 3.3 % corresponds to 3.65 W/m^2 for 120 W/m^2.

Long term drift or stability of the transducer (DtPa)
This contribution is 0.6 W/m^2 at 120 W/m^2.

Directional response error as a function of the azimuth and zenith angle (Rd)
Using the equations presented in [10, chapter 5.4], the incident angle, representative for the diffuse radiation, is 56.93° for a collector tilt angle of 29°.
Thus we can use the maximal uncertainties for incidences angles lower than 60° of ± 2 % specified by the 120 W/m^2. This corresponds to 2.4 W/m^2 related to 120 W/m^2.

Offset errors
Same considerations as above

Temperature dependence of the sensitivity (Dter)
The uncertainties due to a temperature gradient correspond to ± 1.2 W/m^{2}at 120 W/m^2.

Non linearity (NL)
The uncertainty due to the non linearity of 0.6 % is ± 0.72 W/m^2 relative to the normalized diffuse irradiance.

Spectral response (Es)
Using the same calculation as for the global radiation, we get an uncertainty of ± 0.6 W/m^2 at 120 W/m^2.

Tilt response error (MIn)
The tilt response error at 120 W/m² is assumed to be ± 0.24 W/m^2.

Resolution of the measuring unit HP34970A
This uncertainty is ± 0.01 W/m^2 for 120 W/m². As this error appears in a strictly random form, it has not to be considered as systematic error.

Long term drift of the measuring unitHP34970A (DtS) At 120 W/m² the drift causes uncertainties of ± 0.012 W/m^2 and ± 0.2 W/m^2 that sum up to 0.21 W/m^2.

Error of the A/D converter of the HP34970A (AD)
Using the same assumptions as for the global radiation the uncertainty caused by the A/D conversion may be characterized by an error of 0.02W/m^2. This may be considered as conservative, as the diffuse irradiance in generally lower than the global radiation.

Systematic uncertainties by the application of the diffuse radiation correction model (DEH)
The diffuse radiation correction is subject to uncertainties. In [11] a root mean square error of ± 12 W/m^2 for the hourly mean values under all sky conditions (conditions without any data selection criterions) was observed for the application of the Drummond diffuse radiation correction model [26]. For the site under inspection a root mean square error RMSE of 3.45 W/m^2 and mean bias error of 0.1 W/m^2 , was observed [16] under all sky conditions for the one hour mean values of the horizontal diffuse irradiance using the model given by Dehne [17]. For the tilted diffuse irradiance used here, we using the Dehne diffuse radiation correction model that was developed for the horizontal diffuse radiation, considering the same root mean square error and mean bias error as above. For the uncertainty budget, only the MBE as systematic error has to be considered (see introduction). The RMSE is considered as random error. Although the application of the correction model can led to different MBE and RMSE for different clear sky indexes [11] in this article we only considerate all sky conditions for these errors according to their small amplitude [16].

Application of the diffuse radiation correction model (CMU)
In case that a shadow band is used for blocking the direct irradiance, the irradiance signal of the shaded (diffuse) pyranometer has to be corrected for the diffuse radiation blocked by the shadow band. If no correction is applied, it can lead to the monthly averaged error of horizontal diffuse irradiance measurement of up to 24 % [11] that corresponds to 28.8 W/m^2.

EVALUATION OF THE UCERTAINTY BUDGET FOR THE DIFFUSE IRRADIANCE

Table 2 shows the uncertainty budget determined for the magnitude of the diffuse solar radiation that is specified by the EN12975 for the normalized efficiency curve (120 W/m2). For table 2 the same general calculations as for table 1 are considered. The application of the shadow ring correction model according to Dehne results in a monthly mean correction of 28 W/m^2 that is presented in table 2 as correction. Other corrections methods may be applied to reduce systematic errors sources of the diffuse [28] and global [12] irradiance measurements.

Table 2: Uncertainty budget for the measurement of the diffuse radiation at 120 W/m2 with the CM11 pyranometer

origin of the uncertainty		systematic corrections with a model	not corrected systematic uncertainties				
symbol	description of the uncertainty		gross value [W/m²]	distribution form	divisor	u [W/m²]	ν
Cal	Calibration uncertainty		3.65	normal	2.00	1.83	∞
DtPa	Drift over time (change / year)		0.60	uniform	1.73	0.35	∞
Rd	directional response (as a function of the azimuth and the zenith angle)		2.40	uniform	1.73	1.39	∞
OS I	Offset originated by the thermal radiation		7.00	uniform	1.73	4.04	∞
OS II	Offset originated by the temperature change		2.00	uniform	1.73	1.15	∞
Dter	Temperature dependence of the sensitivity		1.20	uniform	1.73	0.69	∞
NL	Non linearity		0.72	uniform	1.73	0.42	∞
ReE	Spectral response		0.60	uniform	1.73	0.35	∞
MIn	Tilt response		0.24	uniform	1.73	0.14	∞
DtS	Long time drift of the measuring system		0.21	uniform	1.73	0.12	∞
A/D	Error of the analog to digital converter of the measuring unit		0.02	uniform	1.73	0.01	∞
DEH	Uncertainties obtained by the application of the correction model		0.10	uniform	1.73	0.06	∞
CMU	Monthely correction with the shadow band correction model	28.8		uniforme	1.73	0.00	∞
	Combined correction	**28.8**					
	Combined standard uncertainty			**normal**		**4.88**	∞
	Expanded standard uncertainty			**normal**		**9.77**	

APPLICATION: PRYRANOMETER UNCERTAINTIES IN THE FRAMEWORK OF COLLECTOR PARAMETER IDENTIFICATION BY A QUASY DYNAMIC COLLECTOR TEST

The model of a solar thermal collector has to describe its efficiency as function of irradiance, ambient and operational temperatures. Eqn. (4) gives the respective model that is applied in the framework of the EN1295 and specifies the QDT collector test. This model takes into account thermal losses, showing a linear and quadratic dependence on the temperature difference (ΔT) between the average absorber temperature T_m and the ambient temperature T_a (4th and 5th term of eqn.4). Optical losses are taken into account by the fist 3 terms of this equation. The first term gives the response to normal incidence beam radiation, the second term handles the variation of the loss effects of non normal incidence by an incidence angle modifier of the beam irradiance, the third term handles the incidence angle effects for the diffuse irradiance, characterized by a unique modifier $K_{\theta d}$. The incidence angle effects for the beam irradiance are summarized by an incident angle modifier function $K_{\theta b}(\theta)$ (eqn. 4), θ being the incidence angle and $K_{\theta b}(\theta)$ is given by $K_{\theta b}(\theta) = 1 + b_0\ (1/\cos(\theta)-1)$. To account for slightly unsteady operation conditions, the last term in eqn.4 describes the influences of the thermal capacity of the collector.

The regression variables used in equation (4) are labeled as X_1 to X_6 and the regression coefficients as a_1 to a_6.

$$\eta_{\mathrm{mo}} = \overbrace{\underbrace{\overbrace{\eta_0^*}^{a1}\ \overbrace{\frac{G-G_d}{G}}^{X1}}_{\text{beam model}} + \underbrace{\overbrace{\eta_0^*\, b_0}^{a2}\ \overbrace{\left(\frac{1}{\cos\theta}-1\right)\frac{G-G_d}{G}}^{X2}}_{\text{incidence angle model, direct irradiance}} + \underbrace{\overbrace{\eta_0^*\, K_{\theta d}}^{a3}\ \overbrace{\frac{G_d}{G}}^{X3}}_{\text{inc.angle model, diffuse irr.}}}^{\text{beam radiation model} = K\theta b(\theta)\times\eta_0\times(G\text{-}Gd)/G} \underbrace{- \overbrace{k_1}^{a4}\ \overbrace{\frac{\Delta T}{G}}^{X4} - \overbrace{k_2}^{a5}\ \overbrace{\frac{(\Delta T)^2}{G}}^{X5}}_{\text{heat loss properties}} - \underbrace{\overbrace{k_3}^{a6}\ \overbrace{\frac{dT_m}{d\tau}\cdot\frac{1}{G}}^{X6}}_{\text{thermal capacity property}}}^{\text{optical properties}} = \eta_{\mathrm{me}} = \frac{\dot{m}\, c_p\,(T_{out}-T_{in})}{G\,A}$$

(4)

The regression coefficients a_1 to a_6 that have to be determined by the regression process are: a_1 [unitless] - the not normalized zero loss efficiency η_0^* of the QDT, a_2 [unitless] – the scale factor for the incidence angle modifier of the beam radiation, determined by $a_2 = \eta_0^* \cdot b_0$, a_3 [unitless] – the incidence angle modifier for diffuse radiation determined by $a_3 = \eta_0^* \cdot K_{\theta d}$, a_4 – the linear heat loss coefficient k_1 [W/(m² K)], a_5 the quadratic heat loss coefficient k_2 [W/(m²K²)] and a_6 – the coefficient for

the thermal capacity k_3 [J/(m^2 K)]. Multiplying the eqn. (4) with the global radiation G and dividing the result by the collector area, one obtains the modeled collector power $\dot{Q}_{mo}$ and the measured collector power $\dot{Q}_{me}$ per square meter collector area.

In the QDT regression the measured variables that determine the regression variables X_1 to X_6 are: The global irradiance G [W/m^2], the diffuse irradiance G_d [W/m^2], the incidence angles θ [°], the mean temperature difference, calculated by the difference of the mean collector temperature $T_m = T_{in}/2 - T_{out}/2$ and the ambient temperature T_a, where T_{in} is the inlet - and T_{out} is the outlet temperature, the temperature variations $\hat{\partial} T_{m,}$ of T_m in the measuring interval and the measuring interval $d\tau_i$ [s] that , according to [1] maybe set to 1 to 6 seconds. In the case discussed here 5 min intervals are applied. In the regression the measured mean values of the efficiency values η_{me} are set as a goal for the efficiency values estimated by the model η_{mo} (eqn.4) [1], where c_p is the effective heat capacity of the fluid passing the collector (that is a function of the mean collector temperature), $\dot{m}$ is the mass flow of the fluid and A is the collector aperture area.

REGRESSION ANALYSIS

As it is shown in [2] for the SST and in [1] for the QDT classical least square regression techniques may be used to derive both the regression coefficients and their uncertainties. The basis for the regression procedure is given by the equation for the error sum of square SS_E (eqn. 5) of the difference of the measured and the model efficiency, which has to be minimized. For the QDT model one may write:

$$SS_E = \sum_{i=1}^{n} (\in_i)^2 \rightarrow \min = \sum_{i=1}^{n} \left(\eta_{me,i} - \eta_{mo,i} \right)^2 = \sum_{i=1}^{n} \left(\eta_{me,i} + \sum_{j=1}^{p} \left(X_{i,j} \ \hat{a}_j \right) \right)^2 \quad (5)$$

Where the indices j = 1 to p count the model variables that is the same as the number of regression coefficients for regressions without intersections (p is 6 for the QDT) and i = 1 to n the samples of the variables [19].

Observation: In [27] the p value specifies the number of regression coefficients like p = k + 1, where k specifies the number of the regression variables. In the regressions without intersections k is equal to p and therefore in the present article only the p-value is used for the resented equations.

The regression coefficients $\hat{a}_1$ to $\hat{a}_p$ for the QDT, estimated with sample or test data, may be identified by solving the linear regression model (eqn. 5), which is given in equation (6) as matrix expression. With the regression coefficients, the modeled efficiency for the time i can be calculated with

$$\eta_{mo,i} = \sum_{j=1}^{p} \hat{a}_j \ X_{i,p} \quad (6)$$

The regression variables used are $X_{i,j}$ (see also eqn.4). In equation (7) the $y_1 \ldots y_n$ [unitless] represent the estimated efficiency values, $\in_1 \ldots \in_n$ [unitless] the residues given by the differences between $\eta_{mo,i}$ and $\eta_{me,i}$, n is the number of mean values in a sample or collector test, j = 1…p counts the number of regression variables and $x_{11} \ldots x_{np}$ defines the sample of the measured variables.

-

$$\hat{y} = \eta_{mo} = [X] \cdot \hat{a} + \in = \begin{bmatrix} y_1 \\ y_2 \\ \vdots \\ y_n \end{bmatrix} = \begin{bmatrix} x_{11} & x_{12} & \cdots & x_{1k} \\ x_{21} & x_{22} & \cdots & x_{2k} \\ \vdots & \vdots & \ddots & \vdots \\ x_{n1} & x_{n2} & \cdots & x_{np} \end{bmatrix} \cdot \begin{bmatrix} \hat{a}_1 \\ \hat{a}_2 \\ \vdots \\ \hat{a}_p \end{bmatrix} + \begin{bmatrix} \in_1 \\ \in_2 \\ \vdots \\ \in_n \end{bmatrix} \quad (7)$$

The estimation of the residual mean square error $E(\sigma^2)$, also named MSE, represented by a data sample, is given by eqn. (8), using reduced matrix/vector expression for a collector test:

$$E(\sigma^2) = \frac{\sum_{i=1}^{n} (\in_i)^2}{n-p} = \frac{\left(y - X \cdot \hat{a}\right)' \left(y - X \cdot \hat{a}\right)}{n-p} \quad (8)$$

Using these mean square errors and the data matrix X, according to [19] the estimated variances of the coefficients $E[\mathrm{var}(\hat{a}_j)]$ are obtained for a collector test as diagonal elements of the matrix given in eqn. (9). The off diagonal elements of these matrixes refer to the estimated covariances of the estimators $E[\mathrm{cov}(\hat{a}_j, \hat{a}_j)]$.

$$E(\sigma^2) \left(X' \cdot X\right)^{-1} = \begin{bmatrix} E[\mathrm{var}(\hat{a}_0)] & E[\mathrm{cov}(\hat{a}_0, \hat{a}_2)] & \cdots & E[\mathrm{cov}(\hat{a}_0, \hat{a}_p)] \\ E[\mathrm{cov}(\hat{a}_2, \hat{a}_0)] & E[\mathrm{var}(\hat{a}_2)] & \cdots & E[\mathrm{cov}(\hat{a}_2, \hat{a}_p)] \\ \vdots & \vdots & \ddots & \vdots \\ E[\mathrm{cov}(\hat{a}_p, \hat{a}_0)] & E[\mathrm{cov}(\hat{a}_p, \hat{a}_2)] & \cdots & E[\mathrm{var}(\hat{a}_p)] \end{bmatrix} \quad (9)$$

We thus obtain the standard error of the estimated regression coefficients $E[s_e(\hat{a}_j)]$ that are calculated for each data sample or collector test by the square root of diagonal elements of this matrix (eqn. 9) with the following equation

$$E\left[s_e\left(\hat{a}_j\right)\right] = \sqrt{E[\mathrm{var}(\hat{a}_j)]} \quad (10)$$

Table 1 shows the determined collector coefficients, and there uncertainties, whereby the regression coefficients uncertainties [5] are calculated by the following equation

$$U(\hat{a}_j) = t_{\alpha/2,n-p} \ s_e(\hat{a}_j) \quad (11)$$

Where $t_{\alpha/2,n-p}$ is the *student-t value*, used to calculated the two sided confidence interval of $U(\hat{a}_j)$ with (1-α)100% of confidence and n-p degrees of freedom, where n is the quantity of the used mean values and p is the quantity of the

regression coefficients for the linear regression without intersection.

Table 1: Regression results of the quasi-dynamic collector test

QDT N° 1				
regression coefficients	$\hat{a}_j$	$E[s_e(\hat{a}_j)]$	$Uc(\hat{a}_j)$	units
$\hat{a}_1$	0.655	0.003	0.006	[-]
$\hat{a}_2$	-0.092	0.012	0.024	[-]
$\hat{a}_3$	0.624	0.004	0.008	[-]
$\hat{a}_4$	5.236	0.180	0.355	[W / m² K]
$\hat{a}_5$	0.042	0.003	0.007	[W / m² K²]
$\hat{a}_6$	12.367	0.496	0.978	[kJ / m² K]
QDT N° 1				
collector coefficients	Cc	U(Cc)	units	U(Cc) %
η_{0_norm}	0.647	0.006	[-]	0.99
b_0	-0.140	0.037	[-]	-26.55
$K_{\theta d}$	0.953	0.016	[-]	1.66
k_1	5.236	0.355	[W / m² K]	6.79
k_2	0.042	0.007	[W / m² K²]	16.07
k_3	12.367	0.978	[kJ / m² K]	7.91

NORMALIZED EFFICIENCY CURVE WITH ITS REGRESSION UNCERTAINTIES

Setting up the normalized values of the incidence angle (15°), diffuse radiation (120 W/m^2) and global radiation (800 W/m^2), as well as the collector coefficient values in equation (4) and varying only the ΔT values, we draw the normalized efficiency curve. For this curve the dT_m value is set to zero, because the normalized efficiency curve is considered for a steady state condition. The uncertainty of the efficiency curve is calculated with the following equation

$$U(\eta)_i = \pm t_{\alpha/2,n-p}\sqrt{E(\mathrm{var}(\eta_i))} = \pm t_{\alpha/2,n-p}\sqrt{\sigma^2\left\{X_{i,0}\right\}\left[[X]^T[X]\right]^{-1}\left\{X_{i,0}\right\}^T} \quad (12)$$

Where [X] is the matrix composed of the regression variables. The columns of this matrix X_{11} at X_{np} are determined by the variables used for the regression (eqn.7). The vectors $\left\{X_{i,0}\right\}$ are built up of the rows X_{11} to X_{16} up to X_{n1} to X_{n6} determined by the variables as used to define the normalized efficiency curve (compare eqn. 7). For the variable X_1 to X_5 the global radiation of 800 W/m^2 and the diffuse radiation of 120 W/m^2 are used. The temperature difference ΔT is varied from (0 to 80) K. To include also the uncertainty that may be caused by the dynamic part of the model, as worst case assessment the maximal 5 min mean value of ΔT_m , as occurred in the measurements, the global radiation of 800 W/m^2 and the time interval of dτ are considered for the X_6 values in the column 6.

COMBINING THE REGRESSION UNCERTAINTIES WITH THE PYRANOMETER UNCERTAINTIES IN THE NORMALIZED EFFICIENCY CURVE

As the systematic pyranometer uncertainties can not be corrected, as discussed above, they have to be explicitly included in the uncertainties of the test results. As the two instruments for the global and the diffuse irradiance are measuring independent, the expanded uncertainty of the efficiency curve has to be determined by a combined uncertainty calculation [4].

From eqn. (4) and the calculation of the measured efficiency values η_{me} one can see that the global irradiance measurements effects both the measured and the modeled efficiencies. Thus, within the regression process all the systematic and random uncertainties in this term are annulated. The same effect happens by the regression using the measured and modeled collector power values [18]. Therefore we have to determine the combined efficiency uncertainties without the consideration of in the radiation in the denominator of eqn. (4). As consequence, the uncertainties in the calculated collector efficiency η_{mo} can be calculated as shown in equation (12), using the uncertainty of the calculated collector power $\dot{Q}_{mo}$ (given here as specific power per collector area in W/m²)

$$U(\eta) = \sqrt{\left(\frac{\partial(\dot{Q}_{mo})}{\partial(G)}\frac{U(G)}{G}\right)^2 + \left(\frac{\partial(\dot{Q}_{mo})}{\partial(G_d)}\frac{U(G_d)}{G}\right)^2 + U^2(\eta_r)} \quad (12)$$

where $U(\eta,G)$ and $U(\eta,G_d)$ are the uncertainties in the collector power originated by the global and diffuse radiation measurements, $U(\dot{Q}_{mo},G)$ and $U(\dot{Q}_{mo},G_d)$ are the uncertainties in the collector power originated by the global and diffuse radiation measurements and $U(\eta_r)$ are the uncertainties originated by the regression process.

The results are given in Figure 1. It shows the uncertainties estimated from the regression process - assuming no uncertainty in the radiation measurement-U1 and the expanded uncertainties U2 that are determined by the regression and pyranometer uncertainties.

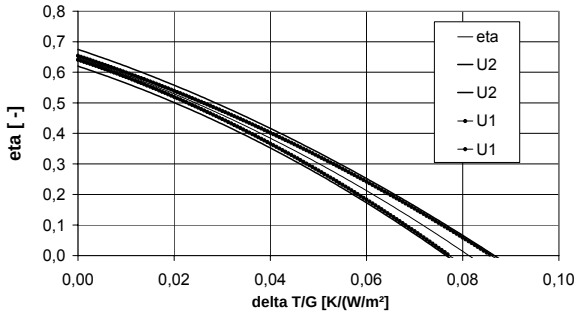

Figure 1: Normalized efficiency curve (middle line) with the expanded (U2, max value is the upper- and min value is the lower line) and the regression uncertainties (U1, max value is the 2nd line from the top, min value is the 2nd line from the bottom)

SUMMARY AND OUTLOOK

This article discusses the fact, that the uncertainties of the result of a collector test are not only those given by the analysis of the uncertainties of the regression process that are caused by the random errors of the measurements, but are

also effected by systematic – but unknown - errors of the radiation sensors. We have demonstrated this by focusing on the irradiance transducers (pyranomters) used in the test. The European- and International Standard determine secondary standard pyranometers for the radiation measurements. The uncertainties of a Kipp & Zonen CM11 pyranometer, which is classified as secondary standard pyranometer [6], enlarge the collector test uncertainties remarkably for low operation temperatures (Figure 1).

This calls for either the use of other transducers or higher standards. One possibility is to use a pyranometer of higher standard (e.g. K&Z CM 22, secondary standard) or a pyrheliometer measuring the direct irradiance and calculating the global radiation from the sum of direct and diffuse radiation. The second suggestion is motivated by the fact that the measurement of a pyrheliometer is less dependent to the influence of different ambient conditions than a pyranometer.

On the other hand one may use effort for analyzing and correcting some of the systematic pyranometer uncertainties. Suggestions in this direction are e.g. given by [12] for the global radiation measurement and by [22] for the calibration of a diffuse pyranometer. For the global radiation the expanded uncertainty may be considerably reduced by reducing the traceable calibration uncertainty. If this uncertainty is reduced from 3.03% to 0.6 % [31], the expanded uncertainty for global radiation is reduced from 29.83 W/m^2 to 19.85 W/m^2. For the diffuse radiation the expanded uncertainty may be considerably reduced by reducing the offset error originated by the thermal radiation. If this error is reduced from 7 W/m^2 to 4 W/m^2 [28], the expanded uncertainty for diffuse radiation is reduced from 9.77 W/m^2 to 7.2 W/m^2. Other prerequisites are the detailed analysis of the measurement of the diffuse irradiance for the tilted plane, notably in applying shadow-band corrections and the detailed analysis of the uncertainty originated by the variations of the sensitivity as a function the solar spectrum for the used pyranometer.

SYMBOLS

a_j	regression coefficient
b_0	incident angle modifier coefficient [unitless]
c_p	effective heat capacity of the fluid [J/(kg K)]
D_f	diffuse fraction [unitless]
error	measured minus modeled collector efficiency [unitless]
G	global solar irradiance [W/m^2]
G_d	diffuse solar irradiance [W/m^2]
G_b	beam solar irradiance [W/m^2]
$j = 1..p$	number of the used model components
$i = 1..n$	number of the mean values used for the regression
k_1	linear heat loss coefficient [W/(m^2 K)]
k_2	quadratic heat loss coefficient [W/(m^2 K^2)]
k_3	effective thermal collector capacitance [J/(m^2 K)]
$K_{\theta b}(\theta)$	incidence angle modifier for direct radiation [unitless]
$K_{\theta d}$	incidence angle modifier for diffuse radiation [unitless]
$\dot{m}$	mass flow [kg/s]
n	number of mean values used for the regression
p	number of the used model components, regression coefficients and regression variables
T_{in}	inlet temperature
T_{out}	outlet temperature
T_m	mean collector temperature
T_a	ambient temperature
$t_{\alpha/2,n-k}$	Student-t factor for the level of significance of 100%(1-α) for a two sided confidence interval used for the regresion result
$t_{\alpha/2,n-1}$	Student-t factor for the level of significance of 100%(1-α) for a two sided confidence interval used for to estmate the extended uncertainty of a continuos quantity
u	standard uncertainty
U	expanded uncertainty
$var(a_j)$	variance of the collector coefficient (corresponds also to the squared standard error s_e^2 of a_j)
$X_{i,j}$	regression variable
(1-α)	significance for the statistical tests and the uncertainty estimations
ΔT	difference between collector mean and ambient temperature
η_{me}	measured efficiency value
η_{mo}	modeled efficiency value
η_0	zero loss efficiency at normal incidence [unitless]
η_{0_norm}	η_0 of the QDT normalized to the SST conditions [unitless]
θ	incident angle of the beam radiation [°]
σ^2	residual mean square error [W

REFERENCES

1. CEN Standard 12975-2 (1997). Solar thermal systems and components - Solar collectors – Part 2: Test methods, European Committee for Standardisation.
2. ISO Standard 9806-1(1994). Test Methods for Solar Collectors, Part 1: Thermal Performance of Liquid Heating Collectors Including Pressure Drop. ISO, Switzerland.
3. ASHRAE 93-86 (1986). Methods of Testing to Determine the Thermal Performance of Solar Collectors, American Society of Heating, Refrigeration, and Air-Conditioning Engeneers, Inc.,Atlanta, U.S.A.
4. Kratzenberg (2005), Método para avaliação de incertezas de ensaios de coletores solares baseados nas normas EN12975 e ISO 9806, Master Thesis,

Universidade Federal de Santa Catarina, Florianópolis, Brazil.

5. ISO-GUM(2003) – International Organization for Standardization Guia para a expressão da incerteza de medição. 3 ed. brasileira: INMETRO, ABNT,SBM 120p. Edição revisada Original: ISO-GUM, Guide to the expression of uncertainty in measurement -1993.
6. Kipp & Zonen (2000) Instruction manual CM11 & CM14 pyranometer / albedometer, Kipp&Zonen, Delft, Holland, v. 1104, 66 p.
7. Inmetro (2000) – Instituto Nacional de Metrologia, normalização e qualidade industrial, Vocabulário internacional de termos fundamentais e gerais de metrologia – Original: ISO-VIM *International vocabulary of basic and general terms in metrology* 2ª ed. Brasileira, Brasília.
8. Ifeachor E.C. and Jervis B.W.(1993), Digital signal processing - A practical approach, Addison- Wesley Publishers Ltd.
9. ISO – International Organization for Standardization. ISO 9847; Solar Energy - Calibration of field pyranometers by comparison to a reference pyranometer 1992.
10. Duffie J.A. Beckman W.A. (1991) Solar Engineering of Thermal Processes, Second Edition, John Wiley & Sons, Inc., New York, U.S.A. 919 p.
11. Muneer T. X. Zhang, A new method for correcting shadow band diffuse irradiance data, Journal of Solar Energy Engineering, ASME American society of mechanical engineers. 2002.
12 Lester A, Myers D.R. (2005) A method for improving global pyranometer measurements by modeling responsivity functions, Solar Energy, Volume 80, Issue 3, March 2006, Pages 322-331.
13 Agilent- Users Guide, Agilent 34970A, Data Acquisition / Switch Unit, 1997
14 ISO9060 (1990) – International Organization for Standardization.- Specification and classification of instruments for measuring hemispherical solar and direct solar radiation, Genève Switzerland..
15 Myers, D. R., I. Reda, S. Wilcox, A. Andreas,. (2004) Optical Radiation Measurements for Photovoltaic Applications - Instrumentation Uncertainty and Performance, 50th Annual Conference of the Society of Photo-optical Instrumentation Engineers, Organic Photovoltaics V. Vol 5520. Denver, CO: SPIE Bellingham, Washington.
16 Abreu S. L. Colle S. Almeida A. P. (1999) Determinação de um fator de correção para a radiação solar difusa medida com anel de sombreamento, XV Congresso de Engenharia Mecânica, São Paulo, 9p.
17 Dehne, K. (1984.) Diffuse solar radiation measured by the shade ring method improved by a correction formula, Report n. 15 World Meteorological Organization, Geneva, Suíça
18 Kratzenberg M.G., Beyer H., Colle S. Albertazzi A.G., Güths S., Fernandes D. 1, Oikawa P.M.V., Machado R.H., Petzoldt D. Analysis of the collector test procedures for steady-state and quasi-dynamic test conditions in view of the collector coefficients uncertainties and model stability, Solar World Congress Orlando, Florida, ISES International Solar Energy Society, 2005. 13 p.
19 Montgomery D.C. and Peck E.A. Introduction to linear Regression Analysis Arizona State University John Wiley & Sons, Inc., New York, U.S.A., 1992, 527 p.
20 World Climate Research Programme, Baseline Surface Radiation Network (BSRN), Operations Manual, Version 2.1 L.J.B. McArthur, 2005, 188p.
21 International Organization for Standardization, 1993. Solar Energy—Calibration of a Pyranometer using a Pyrheliometer. ISO 9846, Geneva.
22 Reda, I., Stoffel, T., Myers, D., 2003. A method to calibrate a solar pyranometer for measuring reference diffuse irradiance. Solar Energy 74(2), 103–112.
23 Forgan, B. W., "A New Method for Calibrating Reference and Field Pyranometers", Journal of Atmospheric and Oceanic Technology, vol. 13, pp. 638-645, 1996.
24 Kipp&Zonen (2002) Calibration Certificate, Pyranometer mode CM22, serial number 020072, Manufacturer Kip & Zonen, Röntgenweg 1, Delft, Holland
25 Berk, A., et al., "MODTRAN4 radiative transfer modeling for atmospheric correction," *SPIE Proceedings, Optical Spectroscopic Techniques and Instrumentation for Atmospheric and Space Research III*, Vol. 3756, pp. 348-353, Society for Photo - Optical Instrumentation Engineers, Bellingham, 1999.
26 Drummond, A. J., 1956, On the measurement of sky radiation, Arch. Meteor. Geophys. Bioklim. 7, pp. 413-436.
27 Douglas C. Montgomery and Runger G.C. (2003). Applied Statistics and Probability for Engineers, Chapters 10 and 12, Appendix A, Table II and Table IV, Arizona State University, John Wiley & Sons, Inc., New York, U.S.A..
28 Dutton, E. G., J. J. Michalsky, T. Stoffel, B. W. Forgan, J. Hickey, D. W. Nelson, T. L. Alberta, and I. Reda, 2001: Measurement of broadband diffuse solar irradiance using current commercial instrumentation with a correction for thermal offset errors, Journal of Atmospheric and Oceanic Technology Vol.18, 18p.
29 Myers, D.R.; Stoffel, T.L.; Wilcox, S.; Reda, I.; Andreas, A. Recent Progress in Reducing the Uncertainty in and Improving Pyranometer Calibrations." American Society of Mechanical Engineers (ASME) Journal of Solar Energy Engineering; 2002; 124: pp. 44-50
30 O. 5th ed. OMM no. 8. Guide to meteorological instruments and methods of observation vol. 8. Geneva, Switzerland: Secretariat of the World Meteorological Organization; 1983.
31 Myers, D.R.; Reda, I.; Wilcox, S.; Stoffel, T.L. Uncertainty analysis for broadband solar radiometric instrumentation calibrations and measurements: An Update, World Renewable Energy Congress VIII Denver, Colorado, 2004 ,

